

Special  
Collection

# Recycling of Primary Lithium Batteries Production Residues

M. Kahl,<sup>[a]</sup> S. Pavón,<sup>[a]</sup> and M. Bertau\*<sup>[a]</sup>

Production waste of primary lithium batteries constitutes a considerable secondary lithium feedstock. Although the recycling of lithium batteries is a widely studied field of research, the metallic residues of non-rechargeable lithium battery production are disposed of as waste without further recycling. The risks of handling metallic Li on a large scale typically prevent the metal from being recycled. A way out of this situation is to handle Li in an aqueous solution, from where it can be isolated as  $\text{Li}_2\text{CO}_3$ . However, the challenge in hydro-metallurgical treatment lies in the high energy release during dissolution and generation of  $\text{H}_2$ . To reduce these process-related risks, the Li sheet metal punching residues underwent

oxidative thermal treatment from 300 to 400 °C prior to dissolution in water. Converting Li metal to  $\text{Li}_2\text{O}$  in this initial process step results in an energy release reduction of ~70%. The optimal oxidation conditions have been determined by experimental design varying three factors: temperature, Li metal sheet thickness, and residence time. With  $96.9 \pm 2.6\%$  almost the entire Li amount is converted to  $\text{Li}_2\text{O}$ , after 2.5 h treatment at 400 °C for a Li sheet thickness of 1.99 mm. Final precipitation with  $\text{CO}_2$  yields  $85.5 \pm 3.0\%$   $\text{Li}_2\text{CO}_3$ . Using pure Li sheets, the product  $\text{Li}_2\text{CO}_3$  is obtained in battery-grade quality (>99.5%). Non-precipitated Li is recirculated into the process on the stage of dissolving  $\text{Li}_2\text{O}$ , thus avoiding loss of material.

## 1. Introduction

In recent years lithium supply has experienced increasing attention owing to e-mobility becoming an alternative to internal combustion engine vehicles, thus giving rise to reducing  $\text{CO}_2$  emissions.

Li-ion batteries have been the major contributors in the electric mobility sector because of their high capacity compared to other energy-storage devices.<sup>[1–5]</sup> For instance, from 1.4 to 3.0 kg of Li are required to drive 60 km in an electric vehicle before a recharge is required.<sup>[6]</sup> Although the main market of Li is batteries (65%), the metal is also needed in the production of aluminum and pharmaceuticals, enamel, glass, ceramics, and lubricating grease.<sup>[4,5,7]</sup> Consequently, the global Li demand has increased considerably reaching 77,200 t of Li or 411,000 t LCE (lithium carbonate equivalents) in 2019.<sup>[7,8]</sup> Estimations for the time until 2027 show an ongoing trend in demand, with a consumption of up to 1,000,000 LCE (188,000 t Li).<sup>[3,9]</sup> Although lithium reserves worldwide in 2019 amounted to 17 million metric tons, supply has been classified critical because 78% of the global production is from Australia and Chile. Added Chinese production, too, 88% of global lithium production is concentrated in these four countries (Figure 1).<sup>[2,7,9]</sup>

In view of the demand in the European Union alone – which in 2050 is estimated to be up to 60 times higher than currently

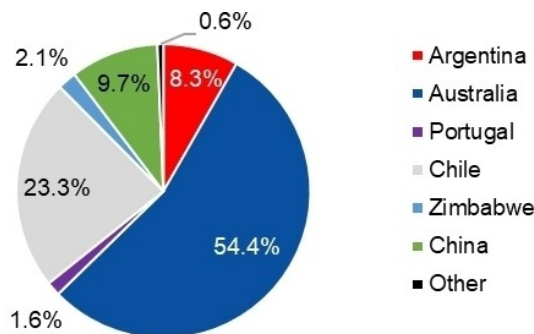


Figure 1. Li global production distribution by country. Data from Ref. [7].

– it is clear why the European Commission has recently declared lithium as critical raw material.<sup>[10]</sup> Hence, a stable lithium supply is indispensable. Therefore, to avoid geopolitical conflicts and to reduce import dependence, domestic lithium recycling from end-of-life (EoL) products and production residues has become crucial. At present, the Li recycling rate from secondary sources is negligible and far below the European action plan on batteries.<sup>[11]</sup> Less than 1% of Li is recycled, which is owed to the economic inefficiency of existing processes.<sup>[2,12,13]</sup> As a result, lithium is disposed of or vanishes in slags when batteries are recycled for more valuable metals, such as cobalt and nickel.<sup>[2,14]</sup> The non-recycled EoL devices are incinerated or landfilled. If the disposal is not carried out correctly serious environmental issues can be caused due to highly toxic of Co.<sup>[15]</sup> Due to the increasing demand of this metal, Sonoc et al. predict a Li-supply crisis for the next decade. To stabilize Li-supply over the coming years the recycling rate has to be increased by 90%.<sup>[13]</sup>

A so far underestimated source for secondary lithium is primary Li batteries, which are not rechargeable, i.e., those with a lithium metal anode. Common battery types are CR 2032 or CR 123. In particular, the metallic production residues represent

[a] M. Kahl, Dr. S. Pavón, Prof. M. Bertau  
Institut of Chemical Technology  
TU Bergakademie Freiberg  
Leipziger Straße 29, 09599 Freiberg, Germany  
E-mail: martin.bertau@chemie.tu-freiberg.de

An invited contribution to a Special Collection on Resource Chemistry

© 2021 The Authors. ChemPhysChem published by Wiley-VCH GmbH.  
This is an open access article under the terms of the Creative Commons Attribution Non-Commercial NoDerivs License, which permits use and distribution in any medium, provided the original work is properly cited, the use is non-commercial and no modifications or adaptations are made.

a valuable resource owing to their high purity and availability in industrialized countries. In Germany for instance, 814 t primary lithium batteries containing Li entered the market in 2019, with the production waste being disposed of.<sup>[16]</sup> However, the high reactivity of Li towards oxygen and nitrogen has been the major reason why Li anode production residues are not recycled. On the other hand, direct reuse would cause problems concerning the high purity demanded.<sup>[17,18]</sup> As a result, production residues are treated as waste and not available for the circular economy. In fact, to the best of our knowledge, no recycling process is known for these production residues. In fact, established processes focus on the processing of *spent* batteries. In one of these, the Recupyl process, the batteries are shredded under an atmosphere of CO<sub>2</sub> and Ar and sieved. The Li rich fraction is dissolved in water. Li is recovered as Li<sub>2</sub>CO<sub>3</sub> by precipitation with CO<sub>2</sub>.<sup>[19]</sup> The Toxco process consists of cryogenic cooling, shredding, and milling as pretreatment. Li is recovered as Li<sub>2</sub>CO<sub>3</sub>, by precipitation with CO<sub>2</sub> after multiple dissolution filtration steps and electrolytic purification.<sup>[20]</sup> There are a series of academic approaches on the laboratory scale, which suffer from several drawbacks, though. Shin et al. proposed a thermal treatment of spent batteries at 300 to 600 °C for 2 h under an Ar atmosphere. After sieving, they receive a metallic powder with 8 w/w.% Li. However, the subsequent processing of this metallic powder is not described, and neither is the recovery of a Li chemical.<sup>[18]</sup> Another process is using a mixture of hydrochloric acid/nitric acid with ratios from 2:1 to 3:1 to leach spent batteries. Nevertheless, a high acid concentration is needed, and there is a considerable amount of leaching residues that needs to be disposed of, not to speak of the costs for acids and neutralization which surpass the intrinsic Li value by far.<sup>[21]</sup> CN104143668 A dissolves the anode material in water forming a slurry, while the recovery or purification of LiOH is not provided.<sup>[20]</sup> WO9859385A1 describes a process for recovering pure LiOH electrolytically generated from battery residues. Further purification is done by nanofiltration.<sup>[23]</sup> EP2450991 A1 reports on a process for metal recovery from spent batteries, where Li is recovered as Li<sub>2</sub>CO<sub>3</sub> after an extensive hydrometallurgical process via precipitation with NaHCO<sub>3</sub> from Li<sub>2</sub>SO<sub>4</sub>. For the latter step alone, 2–4 M sulfuric acid is required. Li yield was 85%. Again, it is evident that process efficiency suffers from the large number of process steps required. To these high operating costs still add the chemicals costs.<sup>[24]</sup> In sum, there exist suggestions for spent batteries, yet there is no solution to recycle lithium anode metal sheet punching residues.

The aim of the process described here is the recovery of lithium from production waste as a lithium salt which is a feedstock for lithium accumulator production (secondary lithium batteries). In contrast to spent batteries, production residues consist of almost pure Li. Li-compounds are contained rather as a trace impurity. Consequently, the biggest challenges are (i) the high energy release (~32 MJ/kg Li, which is sufficient to evaporate 12.4 kg H<sub>2</sub>O) and (ii) H<sub>2</sub> generation during dissolution (1,614.8 LH<sub>2</sub>/kg Li). We therefore developed a process (Figure 2), which circumvents both H<sub>2</sub> generation and heat production through preceding thermal oxidation of Li to

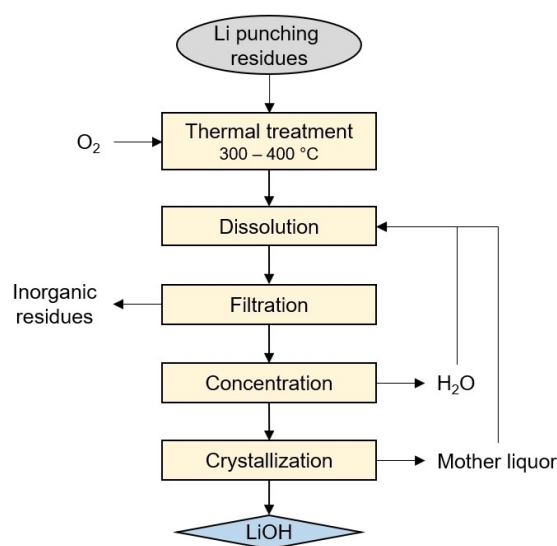
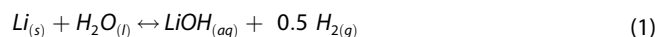


Figure 2. Recycling process scheme of Li battery production residues.

Li<sub>2</sub>O at  $T=300\text{--}400\text{ }^{\circ}\text{C}$ . After the oxidation product has been dissolved in deionized water, the solution is purified by filtration, and eventually, LiOH·H<sub>2</sub>O is obtained by crystallization. As potential residual contaminations have been separated this way, high crude product purity is obtained (battery-grade >99.5%), which does not require further purification. By refunnelling waste lithium (82,000 USD/ton) into the material cycle as high-priced *bg*-LiOH·H<sub>2</sub>O (7,100 USD/ton), the loop is closed, thus contributing to a circular economy. In addition, the process does not require any additional chemicals except for the solvent.<sup>[7,25]</sup> Last not least, the controlled energy release through smooth thermal oxidation is the key to successfully implementing the process on a larger scale.

## 2. Theoretical Background

The dissolution of Li in water is characterized by a high energy release accompanied by hydrogen generation [Eq. (1)]. The energy release makes dissolution difficult to handle and for safety reasons unfeasible on a larger scale.



$$\Delta_{\text{r}}H (25\text{ }^{\circ}\text{C}) = -222.7 \text{ kJ/mol}$$

The dissolution of Li<sub>2</sub>O<sub>(s)</sub> is easier to manage [Eq. (2)]. By converting Li to Li<sub>2</sub>O<sub>(s)</sub>, the energy release upon dissolution is reduced by 70%.



$$\Delta_{\text{r}}H (25\text{ }^{\circ}\text{C}) = -133.3 \text{ kJ/mol}$$

### 3. Results and Discussion

#### 3.1. Characterization of Starting Materials

The residues of primary Li batteries production were different from each other in composition terms. Hence, they were divided into three groups:

- Group A: crumpled metallic residues
- Group B: chads contaminated with stainless steel and plastic
- Group C: metallic rolls contaminated with iodine.

The composition of the samples is given in Table 1. As expected, all samples show a high Li-content, higher than in primary Li-sources or spent batteries. The residues of group A have the highest Li-content and purity and group B the lowest Li-content due to the high content of stainless steel and plastics. But the Li-content of group B is still higher than that of spent batteries. Group A represents the largest fraction of production residues. However, all the samples are in high purity after dissolution in water, even though the Li-content between the three groups is different. The impurities are mostly insoluble and remain in the leaching residue. Therefore, the residues represent a valuable high-quality source for Li. Due to the high Li-content in the samples of Group A, the current investigation is focused on recovering Li from crumpled metallic residues.

#### 3.2. Oxidation

Li readily oxidizes in the presence of air to form  $\text{Li}_2\text{O}$ ,  $\text{Li}_3\text{N}$ ,  $\text{Li}_2\text{CO}_3$  and  $\text{LiOH}$ .  $\text{Li}_2\text{CO}_3$  is known to be the preferred product of weathering of metallic Li. However, the oxidation rate is relatively low, what results in a low efficiency of the oxidation process. Oxidation can be influenced by several parameters such as humidity, the composition of the surrounding atmosphere, temperature, residence time and thickness of Li-sheets.<sup>[26,27,28]</sup> With the surrounding atmosphere being air at ambient temperature ( $T=25^\circ\text{C}$ ), humidity and atmosphere composition were set constant. Temperature, Li-sheet thickness, and residence time were the chosen parameters to be investigated in the current work. At ambient temperature, 2 days are required to completely oxidize a 1 mm thick Li-sheet (Figure 3).

However, the product obtained from weathering at ambient temperature is characterized by a Li-content of 24.1%, which clearly indicated that  $\text{Li}_2\text{CO}_3$  is the preferred product. Bearing in mind that  $\text{LiOH}$ , which is formed from the primary oxidation product  $\text{Li}_2\text{O}$  by reacting with air humidity is an efficient absorber of atmospheric  $\text{CO}_2$ , this outcome was only too natural

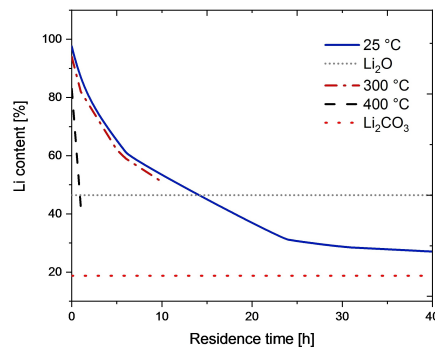


Figure 3. Li-content [%] comparison of different oxidation temperatures.

and was confirmed by XRD studies. Other constituents were  $\text{Li}_2\text{O}$ ,  $\text{LiOH}$ ,  $\text{Li}_3\text{N}$  and  $\text{LiNH}_2$ , from what was obvious that ambient conditions would not suffice for the purpose of Li recycling. Efficient and fast oxidation succeeds at a higher temperature, though. The required ignition temperature is reported to range from 180 to  $640^\circ\text{C}$  depending on humidity and atmosphere composition.<sup>[26]</sup> At  $T=300^\circ\text{C}$  both oxidation rate and oxidation product distribution were almost like that observed at ambient conditions. At  $T=400^\circ\text{C}$  oxidation rates get faster, what is in line with the values reported in literature.<sup>[26,27]</sup> Furthermore, at  $T=400^\circ\text{C}$ , the residence time for the oxidation reaction is reduced from 15 to 1 h.

Based on these experiments the question was whether this approach might be suitable for industrial application. For these purposes, optimized reaction parameters were to be determined by design of experiments.

#### 3.3. Optimization

The optimization of the Li oxidation reaction and the subsequent water leaching was carried out by using the  $3^3$  Box-Behnken experimental design. The investigated factors were: temperature  $T$ , residence time  $t$ , and Li-sheet thickness  $d$ . The target value is Li conversion from metallic Li to  $\text{Li}_2\text{O}$ , which affects the energy release during dissolution. The results of the 15 experiments are depicted in Table 2.

The experiments were successful in terms of almost quantitative conversion of Li to  $\text{Li}_2\text{O}$  and reduced energy release upon dissolving the oxidation product in water. No elemental  $\text{H}_2$  had been formed, the potential occurrence of which had been monitored continuously with a process mass spectrometer.

The experimental error of 1.6 percent points is owed by early oxidation of Li sheets during sample preparation. When the latter was done under Ar atmosphere for control purposes, there were no such effects observed. According to the standardized Pareto diagram (Figure 4), five of nine effects are significant. Only the AC and BC binary correlations are insignificant for the conversion of metallic lithium to  $\text{Li}_2\text{O}$ . The

Table 1. Composition of different Li-Product residues samples.

Sample nr.	Group	Elements	Li-content [%]	Purity [%]
1	A	Li, Na	99.89	99.89
2	A	Li, Na	99.82	99.82
3	B	Li, Na, Fe	59.38	99.85
4	C	Li, Na, I	83.42	99.84
5	C	Li, Na, I	88.89	99.67

results also show that temperature  $T$  has the most prominent impact on oxidation, while residence time  $t$  has none and thickness  $d$  only a small one.

### 3.4. Temperature

Together with its squared correlation,  $T$  has the greatest effect on Li conversion. Temperatures  $< 350^\circ\text{C}$  result in minimal conversion, only. Temperatures  $> 350^\circ\text{C}$  provide an enhanced but incomplete conversion. For fast and complete oxidation, the operating temperature should be equal to or above ignition temperature  $T_i$ .  $T_i$  was determined to be  $400^\circ\text{C}$ . Since maximal conversion was reached here, a further increased temperature would not be reasonable and reduce cost efficiency. Because the melting point of Li is  $180.5^\circ\text{C}$ , reaction conditions at higher temperature might interfere with the oxidation progress by sintering of Li metal fragments. Surprisingly no negative effect of sintering could be observed, Li starts to melt at  $T > 180^\circ\text{C}$ .<sup>[29]</sup> A decreasing Li-conversion caused by reduction of the surface

area did not occur. The maximal conversion and negligible effect of sintering demonstrate the high performance of the oxidation process. Therefore, high temperatures are suitable for the oxidation reaction.

### 3.5. Thickness

The thickness is the second greatest linear factor, which contributes to the Li-conversion. However, it remains at a low level. The quadratic effect and the AB correlation show only a small influence. According to Figure 4, the thickness is the only effect with a negative impact on Li-conversion. Such effect is expected, thinner sheets are easier to oxidize even at a lower temperature, due to beneficial greater surface volume ratio or lower charge density. In addition, the thickness shows a nonlinear effect on Li-conversion with a minimal conversion with a thickness of 1.01 mm because of its lowest surface volume ratio. Thicker sheets have a greater surface volume ratio because they are built up by single layers compressed by hand to the desired thickness. These crumpled sheets show a similar conversion to single sheets. Due to the similar behavior of single and crumpled sheets of the same thickness, it can be concluded that the crumpling shows no or just a small negative effect on the Li-conversion. Thus, an intense shredding is not needed, and the crumpled sheet can be directly oxidized. As a result, contamination by sample preparation is minimized as well as a cost reduction. Regardless of the thickness, all sheets will be completely oxidized within 2.5 h at a suitable temperature. Most sheets are very thin but crumpled and oxidize easily and quickly.

### 3.6. Residence Time

The residence time in linear, square, and binary correlations, is not contributing to maximize the Li conversion by oxidation. This fact indicates that after half an hour oxidation is finished and only  $\text{Li}_2\text{O}_{(s)}$  and  $\text{Li}_3\text{N}$  remain in the oxidation residue. The non-significance of residence time enables high throughput, and it is favorable for an industrial application. A low effect of residence time was expected because the high energy release of oxidation results in autothermal process and enhances the oxidation. Consequently, Li-sheets react quickly to  $\text{Li}_2\text{O}$ .

### 3.7. Leaching

The leaching was conducted to completely dissolve the residue within 15 minutes. Therefore, the process enables a 100% removal of Li from the residue. As a solvent, pure water can be used. However, to neutralize the formed  $\text{LiOH}_{(aq)}$  and to avoid the leaching of contamination from glass beakers due to high pH, nitric acid was used in the lab-scale experiments carried out for the optimization of the oxidation stage. Nitric acid was chosen solely for analytical reasons to avoid potentially present metallic impurities from reacting and precipitating with other

**Table 2.**  $3^3$  Box-Behnken design. The experiments shaded in grey correspond to the replicated central point.

Experiment nr.	Temperature $T$ [ $^\circ\text{C}$ ]	Thickness $d$ [mm]	Residence time $t$ [h]	Li-conversion [%]
1	350	1.01	1.5	34.07
2	350	0.01	0.5	34.87
3	300	0.01	1.5	59.38
4	400	2.01	1.5	91.49
5	350	2.01	0.5	25.35
6	350	2.01	2.5	42.85
7	300	1.01	0.5	19.23
8	350	1.01	1.5	34.36
9	400	1.01	2.5	81.97
10	350	0.01	2.5	69.88
11	400	0.01	1.5	83.23
12	300	1.01	2.5	23.27
13	300	2.01	1.5	26.23
14	400	1.01	0.5	84.44
15	350	1.01	1.5	33.41
16	400	1.99	2.49	94.33
17	400	1.99	2.49	99.49

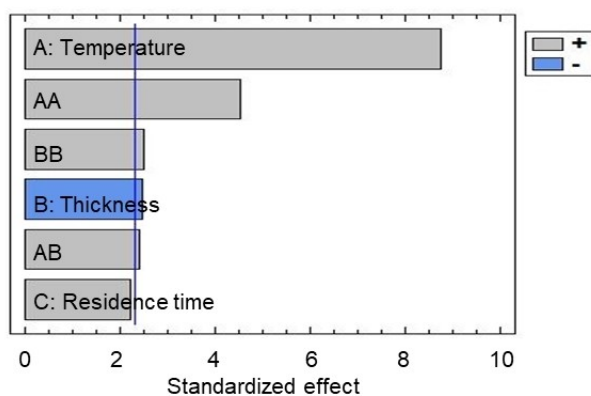


**Figure 4.** Pareto diagram with all the effects influencing Li-conversion (vertical line refers to experimental error).

anions. Unquestionably, However, the use of this reagent should be avoided in order not to increase chemicals costs on an industrial scale pH adjustment will be done with far cheaper sulfuric acid. Li can be recovered directly from the filtrated solution as  $\text{LiOH}_{(s)}$  or as  $\text{Li}_2\text{CO}_{3(s)}$  by precipitation with  $\text{CO}_2$ .

### 3.8. Isolation of $\text{Li}_2\text{CO}_3$

By precipitation as  $\text{Li}_2\text{CO}_3$ ,  $85.5 \pm 3.0\%$  of Li was recovered in single stage precipitation. For complete recovery, a closed loop between dissolution and precipitation for mother liquor is required. The crude product consisted of  $96.7 \pm 0.2\%$   $\text{Li}_2\text{CO}_3$  and  $3.0 \pm 0.2\%$   $\text{LiOH} \cdot \text{H}_2\text{O}$ . Impurities with soda,  $\text{Na}_2\text{CO}_3$ , were  $< 0.1\%$  in all cases. Through final crystallization (Figure 2),  $\text{Li}_2\text{CO}_3$  was obtained in *bg*-quality ( $> 99.5\%$  purity) with  $85.5 \pm 3.0\%$  yield for each precipitation stage. Non-precipitated  $\text{Li}_2\text{CO}_3$  and non-carbonized  $\text{LiOH} \cdot \text{H}_2\text{O}$  remained in the mother liquor and were re-circulated in the process, thus allowing for complete Li recovery as  $\text{Li}_2\text{CO}_3$ .

### 3.9. Model Equation and Optimum

According to the model (Eq. (3)), 99.99% of Li conversion can be reached using the following reaction conditions:  $400^\circ\text{C}$ ; 2 mm and 2.5 h. To validate the model, a twofold experiment was carried out using these parameters.

$$\text{Li-conversion (\%)} = 932.894 - 5.417 \cdot A - 104.905 \cdot B + 6.869 \cdot C + 0.008 \cdot A^2 + 0.211 \cdot A \cdot B + 11.546 \cdot B^2 \quad (3)$$

where:

A: Temperature [ $^\circ\text{C}$ ]

B: Thickness [mm]

C: Residence time [h]

The results of both experiments are shown in Table 2. A Li-conversion of  $96.9 \pm 2.6\%$  was obtained. The Li conversion model optimization yielded a coefficient of determination ( $R^2$ ) of 93.7%.

However, the calculated optimum represents the highest Li-conversion and therefore the lowest energy release during dissolution. Despite the high conversion, the calculated optimum did not represent the best conditions for a technical application, throughput and efficiency are low. Other reaction conditions can enhance the efficiency by decreasing the operational costs and increasing throughput. According to the high influence of the temperature on the Li-conversion and the obtained optimum, this factor has been set-up at  $400^\circ\text{C}$ . Lower thermal lithium oxidation, 72%, is achieved when sheets were 1.2 mm thick and treated for 0.5 h (Figure 5). More than 95% of Li-conversion can be reached at higher residence time for whatever thickness of lithium sheets. To combine the benefits of a high Li-conversion and high throughput and to design an economically viable process, reduction of residence time to 1 h is advisable. To verify the calculated throughput, an experimental set-up of  $400^\circ\text{C}$ , 2 mm and 1 h was conducted, which

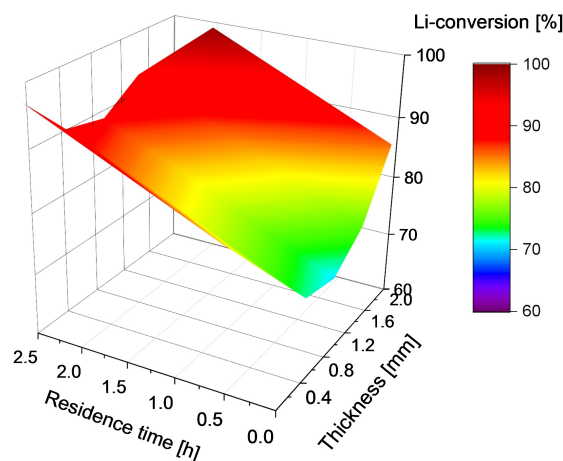


**Figure 5.** Li-conversion [%] calculated by model equation varying the three defined factors.

reached a Li-conversion of  $91.6 \pm 1.6\%$ . As a result, the throughput has increased by a factor of 2.5 compared to the calculated optimum. However, the low significance of punching sheet thickness enables the processing of thicker sheets, thus resulting in less effort and lower costs.

### 3.10. Characterization of Oxidation Product

The oxidation product obtained from thermal oxidative treatment of lithium punching sheets, primarily is not uniform. This is due to the composition of the atmosphere, which is approx. 78%  $\text{N}_2$  and 21%  $\text{O}_2$  with trace amounts of  $\text{CO}_2$ , and additionally  $\text{H}_2\text{O}$  from air humidity. In addition, Li displays an affinity for both  $\text{N}_2$  and  $\text{O}_2$ . The formation of  $\text{Li}_2\text{O}$ ,  $\text{Li}_3\text{N}$ ,  $\text{LiOH}$ ,  $\text{LiOH} \cdot \text{H}_2\text{O}$  and  $\text{Li}_2\text{CO}_3$  was verified by X-Ray Diffraction (XRD) (Figure 6).  $\text{Li}_2\text{O}$  and  $\text{Li}_3\text{N}$  are products of primary oxidation, whereas  $\text{LiOH}$  and  $\text{Li}_2\text{CO}_3$  are secondary products resulting from taking up water and  $\text{CO}_2$ . Since the formation of all compounds contributes to decreasing energy release, the non-uniform composition is not a problem.

$\text{Li}_2\text{O}$  is an effective absorber for  $\text{CO}_2$ . As a consequence, approx. 28.3% of the  $\text{Li}_2\text{O}$  formed are present as  $\text{Li}_2\text{CO}_3$  prior to dissolving the product mixture in water. In fact, instead of theoretically 46.5% Li which were pure  $\text{Li}_2\text{O}$ , a real Li-content of 33.3% was found in the oxidation product. For the overall process, this is beneficial, since the enthalpy of solution is reduced. Instead of  $-133.3 \text{ kJ} \cdot \text{mol}^{-1}$  for the hydration of  $\text{Li}_2\text{O}$ , there is an endothermal contribution of  $90.2 \text{ kJ} \cdot \text{mol}^{-1}$  by  $\text{Li}_2\text{CO}_3$ .

### 3.11. Industrial Application Feasibility

The thermal treatment has been tested successfully on the lab-scale and the high Li-conversion demonstrates the efficiency of the proposed process (Figure 2). The current work focuses on the Li recovery from production residues of group A. There is



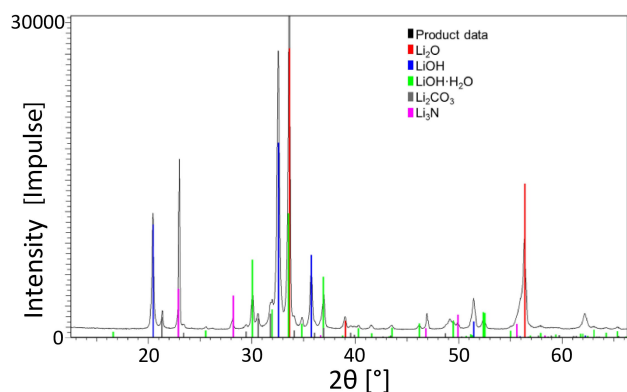


Figure 6. XRD pattern of oxidation product.

no reliable study on the relative amounts of each group in LIB waste till now. However, group A material constitutes the by far major fraction of LIB waste sent to waste management facilities. The samples from group A, B and C mainly differ in the composition of the oxidation product. Considering the impurities present in groups B (mainly Fe) and C (mainly iodine), purification steps are needed to reach high purities of the obtained product. For instance, iron traces ( $>0.1\%$ ) may get into the leachate through partial oxidation when using higher oxidation temperatures ( $\geq 400^\circ\text{C}$ ). Although iron impurities from group B material can be easily separated by precipitation as  $\text{Fe}(\text{OH})_3$ , one has to consider co-precipitation of Li. Since these amounts are low, though, minor losses can be tolerated well. Iodine from group C material, to our experience, leaves the furnaces via the offgas, and thus does not affect the process. Since on a technical scale there is a post-combustion with subsequent offgas-scrubbing the thermal treatment constitutes no environmental issue.

The low significance of residence time enables high throughput, while the effect of thickness allows for abandoning lithium punching sheet pretreatment, such as intense shredding or milling. Several processes, such as Recupyl or Toxco contain shredding in their process scheme, though.<sup>[19,20]</sup> The negligibility of a shredding step simplifies the process and reduces operation costs. The optimal oxidation temperature was  $400^\circ\text{C}$ , which was lower compared to other processes that operate at temperatures up to  $600^\circ\text{C}$ .<sup>[18]</sup> Therefore, the process is less energy intensive. Since the high energy release is transferred from dissolution to oxidation, the energy can be used for autothermal heating.

Due to the usage of high purity production residues, high purity products can be obtained easily. Thus, intense purification steps like those in the Recupyl or Toxco process are not required here.<sup>[19,20]</sup> The impurities in the residues, such as stainless steel and plastic in group B, are insoluble in water and can be conceived of as self-separating upon dissolution. They are removed by filtration. Furthermore, the comparably lower consumption of process chemicals beneficially contributes to the process economy.

In contrast to the approach described here, existing processes are designed to process spent primary or secondary batteries, i.e., they process lithium salts. At present though, there is no such process suited for metallic lithium. In fact, the specific requirements to process materials with high lithium metal content, such as high energy release during dissolution, hitherto has been preventing industrial approaches from coming up. As a solution to all this, the process described here considers these challenges, not only reducing chemicals consumption and enabling full Li-recovery but also providing high crude product purities  $>99.5\%$ .

### 3.12. Safety Considerations

One reason why Li metal so far has not been in the focus of industrial lithium recycling may be safety issues. In fact, both the generation of  $\text{H}_2$  and its strong exothermic reaction with water provoke serious concerns with regard to process safety. Next, till present the non-uniform feedstock compositions of groups A, B and C do not allow for handling the material in one single process. Establishing three different processes with high-safety standards for almost the same, yet slightly differing feedstock qualities renders the entire issue uneconomic. Already storage and transport require safety measures. In fact, the material should be stored under Ar atmosphere to prevent contact with  $\text{O}_2$  and/or  $\text{N}_2$  and moisture, as the uncontrolled exothermic oxidation may cause fires. Simply dissolving the lithium metal sheets in water on first sight appears as the method of choice, yet the formation of an equimolar amount of hydrogen from 1 t of Li metal means  $3,200\text{ m}^3$  of  $\text{H}_2$  (273 K, 100 kPa) to be treated. Once the metal is dissolved, the product is a strongly alkaline solution of LiOH in water, what however is everyday chemistry in industry and can be handled safely.

Our process in contrast, avoids the formation of hydrogen gas to the most possible extent by oxidizing Li-metal in a chamber furnace. At  $T > 350^\circ\text{C}$  the interference with water from ambient moisture is negligible, while the controlled oxidation of the metal in a high-temperature device allows for avoiding the uncontrolled release of reaction heat. Flooding the furnace with argon gas interrupts the reaction on short course, thus providing just another safety option. Potentially generated  $\text{H}_2$  can be removed from the offgas by post-combustion, and offgas treatment in a scrubber prevents environmentally harmful substances from being released to the environment. Of course, there is no experience on the large-scale yet, and these considerations must not be misinterpreted as an all-embracing working safety instruction. These results are the basis for an industrial application, which is presently underway at FNE Entsorgungsdienste Freiberg GmbH, Freiberg, Germany, where the start-up of a demonstration plant is scheduled for mid-year 2021.

## 4. Conclusions

The current recycling process allows for converting metallic Li to  $\text{Li}_2\text{O}_{(s)}$  with a maximal energy release reduction of 70%. The recycling of lithium metal punching residues was optimized using a  $3^3$  Box-Behnken design. A mathematical model was generated, which describes how Li-conversion depends on temperature, thickness of Li-sheets and residence time.

Maximum Li-conversion was determined to be  $96.9 \pm 2.6\%$  for the following reaction conditions: 400 °C; 2 mm and 2.5 h. Furthermore, the Li-purity in the leachate after dissolution reached 99.7%. As expected, temperature shows the greatest effect on Li-conversion. Its linear (A) and squared effect (AA) appear as the top two factors. The non-significance of the residence time facilitates establishing a cost-effective process on an industrial scale. After 30 min, Li oxidation is complete and an oxidation product constituted from  $\text{Li}_2\text{O}$ ,  $\text{Li}_3\text{N}$ ,  $\text{LiOH}$  and  $\text{Li}_2\text{CO}_3$  is received. Regarding punching sheet thickness, the process has been shown to be sufficiently robust to tolerate varying values, what eventually does not require energy intensive shredding and allows for crumpled foils to be used directly.

## Experimental Section

### Starting Material and Sample Preparation

Residues from lithium battery production were supplied by FNE Entsorgungsdienste Freiberg GmbH, Freiberg, Germany and were packed and stored under Ar atmosphere to prevent early oxidation. The elementary composition of the different Li battery production residues was obtained by atomic emission spectrometry with inductively coupled plasma (ICP-OES, Optima 4300 DV, Perkin Elmer, Corporation, Waltham, USA). Structural characterization of obtained products were performed by X-ray diffraction (XRD) analyses (D8 DISCOVER, Bruker, Corporation, Billerica, USA). The device using Cu  $K\alpha$  radiation;  $\lambda = 1.541 \text{ \AA}$ , 40 kV, 40 mA with an opening angle of  $1^\circ 2\theta$ . The XRD patterns were collected with a step of  $0.02^\circ$  and 1 s dwell time.  $\text{H}_2$  evolution was monitored using a process mass spectrometer (Pfeiffer Vacuum QMG 425, Pfeiffer Vacuum Technology AG, Aßlar, Germany).

Sample preparation consisted of deconvolution of crumpled foils and cutting to a size of  $7 \times 7 \text{ mm}^2$ . Single layer thicknesses of deconvoluted sheets were 0.01 mm and 1.01 mm. Thicker sheets were rolled to the desired thickness. Cutting was done under normal air for each sample directly before subjecting to thermal oxidation.

### Oxidation Method

The oxidation experiments were performed in an LVT 15/11 oven (Nabertherm GmbH, Germany) which allows five changes of oven atmosphere per minute. 250 mg of Li-ion battery sample was used for each experiment. The samples were placed in a tempered oven for desired residence time in graphite crucibles.

### Leaching Experiments

The oxidation residues in the optimization stage were leached using 50 mL of nitric acid 1 M for 15 min. Afterwards, the residues

were dissolved completely. The filtrate was analysed by ICP-OES to determine Li yield. Once the optimum was obtained, the complete process was carried out (Figure 2) to verify its possible implementation on an industrial scale. In this case, the leaching of the oxidized residues was done using water to finally obtain  $\text{LiOH}$  without increasing the chemical costs.

### Preparation of $\text{Li}_2\text{CO}_3$

The filtered leaching solution was evaporated to a concentration of 0.05 g/ml (oxidized sample), before  $\text{CO}_2$  was injected for 10 min. The product was recovered by filtration and dried until mass constancy.

### Thermodynamic Values

Enthalpies of reaction and solution were taken from CRC Handbook of Chemistry and Physics.<sup>[30]</sup>

### Optimization

The  $3^3$  Box-Behnken design depicted in Figure 7 was used to optimize the Li-ion battery recycling by determining the global optimum by considering correlations for all binary factor combinations. This design of experiment (DOE) requires tests on every half of the edges and in the centre, which was conducted threefold to determine the experimental error. It varies three factors: temperature  $T$  [°C], thickness  $d$  [mm], residence time  $t$  [h] in a range comprising three levels (Table 3).

The confidential interval was set to 95%. Statgraphics v.18 (Statpoint Technologies, USA) was the software used for statistical evaluation. An ANOVA was conducted to determine which effect contributes significantly to Li-conversion and terms which were not significant were removed by the stepwise method.

The model equation describing how Li-conversion depend on each effect defined previously was obtained by using a multi-linear regression. The influence of the nine effects (linear, squared, and binary correlations) on the Li-conversion were investigated by Eq. (4).

$$y = b_0 + \sum_{i=1}^N b_i x_i + \sum_{1 \leq i < j} b_{ij} x_i x_j + \sum_{i=1}^N b_{ii} x_i^2 \quad (4)$$

where:

$y$ : Target value: Li-conversion

$x_i$ : Factors: temperature, thickness, residence time

$N$ : Number of factors (3)

$b_0$ : Ordinate section

$b_i$ ,  $b_{ij}$ ,  $b_{ii}$ : Regression parameters of linear, squared, and cross effects

## Acknowledgements

Financial support by the German Federal Ministry of Education and Research (Grant nr. 033RK074C) is gratefully acknowledged. Further thanks are owed to Andrea Schneider for conducting ICP-OES analyses and FNE Entsorgungsdienste Freiberg GmbH for

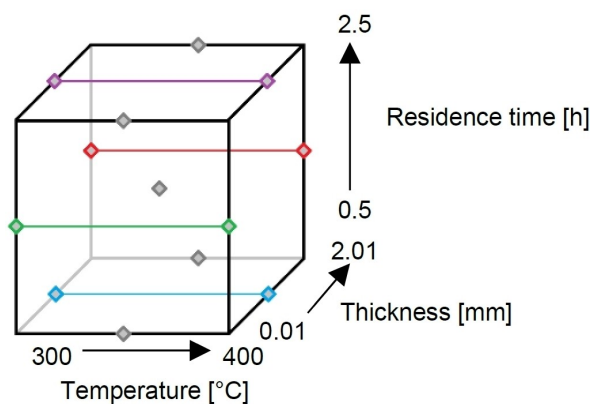


Figure 7.  $3^3$  Box-Behnken experimental design.

Table 3. Factors and levels in the $3^3$ Box-Behnken design.				
Factors		Factor levels		
		-1	0	+1
A	temperature $T$ [°C]	300	350	400
B	thickness $d$ [mm]	0.01	1.01	2.01
C	residence time $t$ [h]	0.5	1.5	2.5

providing Li-ion battery samples. Open access funding enabled and organized by Projekt DEAL.

## Conflict of Interest

The authors declare no conflict of interest.

**Keywords:** Batteries · dissolution · lithium · recycling · thermal treatment

- [1] P. Sood, K. C. Kim, S. S. Jang, *ChemPhysChem* **2018**, *19*, 753–758.
- [2] S. Ziemann, D. B. Müller, L. Schebek, M. Weil, *Resour. Conserv. Recycl.* **2018**, *133*, 76–85.
- [3] Roskill, *Lithium Outlook to 2030*, 17<sup>th</sup> Ed., available at <https://roskill.com/market-report/lithium/>, **2020**.
- [4] G. Martin, L. Rentsch, M. Höck, M. Bertau, *Energy Storage Mater.* **2017**, *6*, 171–179.
- [5] L. Kavanagh, J. Keohane, G. G. Cabellos, A. Lloyd, J. Cleary, *Resources* **2018**, *7*, 57.
- [6] U. S. Geological Survey, *Lithium use in batteries*, Reston, Virginia, **2012**.

- [7] U. S. Geological Survey, *Mineral Commodity Summaries 2020*, Reston, Virginia, **2020**.
- [8] Statista, *Minenproduktion von Lithium nach den wichtigsten Ländern im Jahr 2019*, available at <https://de.statista.com/statistik/daten/studie/159929/umfrage/minenproduktion-von-lithium-nach-laendern/>, **2020**.
- [9] D. C. Bradley, L. L. Stillings, B. W. Jaskula, L. Munk, A. D. McCauley, in *Professional Paper 1802*, (Eds.: K. J. Schulz, J. H. DeYoung, Jr, R. R. Seal II, D. C. Bradley), Reston, VA, **2017**, pp. K1–K21.
- [10] European Commission, *Critical Raw Materials Resilience: Charting a Path towards greater Security and Sustainability*, Brussels, **2020**.
- [11] European Commission, *Building a Strategic Battery Value Chain in Europe*, Brussels, **2019**.
- [12] A. Sonoc, J. Jeswiet, *Procedia CIRP* **2014**, *15*, 289–293.
- [13] C. Peng, F. Liu, Z. Wang, B. P. Wilson, M. Lundström, *J. Power Sources* **2019**, *415*, 179–188.
- [14] GRS Batterien *Die Welt der Batterien*, Hamburg, available at [https://www.grs-batterien.de/fileadmin/Downloads/Welt\\_der\\_Batterien/Welt\\_der\\_Batterien.pdf](https://www.grs-batterien.de/fileadmin/Downloads/Welt_der_Batterien/Welt_der_Batterien.pdf), **2012**.
- [15] S. He, B. P. Wilson, M. Lundström, Z. Liu, *J. Cleaner Prod.* **2020**, *268*, 122299.
- [16] Stiftung GRS Batterien *Erfolgskontrolle 2019*, Hamburg, available at [https://www.grs-batterien.de/fileadmin/Downloads/Erfolgskontrollen/GRS\\_Erfolgskontrolle2019Web.pdf](https://www.grs-batterien.de/fileadmin/Downloads/Erfolgskontrollen/GRS_Erfolgskontrolle2019Web.pdf), **2020**.
- [17] E. P. Kamphaus, S. A. Gomez, X. Qin, M. Shao, P. B. Balbuena, *ChemPhysChem* **2020**, *21*, 1310–1317.
- [18] S. M. Shin, D. W. Lee, C. Y. Kang, J. P. Wang, *Appl. Mech. Mater.* **2013**, *432*, 86–91.
- [19] J. C. Foudraz, F. Tedjar (Recupyl), US7820317B2, **2005**.
- [20] L. Gaines, J. Sullivan, A. Burnham, I. Belharouak, *Transp. Res. Rec.* **2011**, *2252*, 57–65.
- [21] S. Recknagel, A. Richter, *Überprüfung der Schwermetallgehalte von Batterien – Analyse von repräsentativen Proben handelsüblicher Batterien und in Geräten verkaufter Batterien – Erstellung eines Probenahmeplans, Probenbeschaffung und Analytik (Hg, Pb, Cd)*, available at <http://www.umweltbundesamt.de/sites/default/files/medien/publikation/long/3350.pdf>, **2007**.
- [22] X. Chang, K. Cheng, C. Li, W. Wang, Z. Zhou, Z. Zhu, (China Aviat Lithium Battery Luoyang Co Ltd), CN201310532433 A, **2013**.
- [23] J. E. V. Bromme, K.-W. Mok, P. J. Pickering, (Pacific Lithium Limited), WO9859385 A1, **1998**.
- [24] F. Beolchini, G. Furlani, G. Granata, E. Moscardini, F. Pagnanelli, L. Toro, F. Veglio (ECO Recycling s.r.l.), EP2450991 A1, **2011**.
- [25] Euromoney Institutional Investor (Fastmarket), *Latest battery-grade spot lithium prices*, available at <https://www.fastmarkets.com/commodities/industrial-minerals/lithium-price-spotlight>, **2020**.
- [26] D. W. Jeppson, J. L. Ballif, W. W. Yuan, B. E. Chou, *Lithium literature review: lithium's properties and interactions*, USA, **1978**.
- [27] R. A. Rhein, *Lithium Combustion: A Review*, USA, **1990**.
- [28] R. B. Heslop, P. L. Robinson, *Inorganic chemistry: a guide to advanced study*, Elsevier, Amsterdam, **1960**.
- [29] J. O. Besenhard, M. Winter, *ChemPhysChem* **2002**, *3*, 155–159.
- [30] W. M. Haynes, *Handbook of Chemistry and Physics*, CRC Press LLC, Milton, UK, **2016**.

Manuscript received: October 19, 2020

Revised manuscript received: January 5, 2021

Accepted manuscript online: January 19, 2021

Version of record online: February 23, 2021